Numerical modelling of ductile damage mechanics coupled with an unconventional plasticity model

R. Fincato, S. Tsutsumi
University of Osaka, Japan
fincato@jwri.osaka-u.ac.jp, http://orcid.org/0000-0002-2345-6790
tsutsumi@jwri.osaka-u.ac.jp, http://orcid.org/0000-0002-2345-6791

ABSTRACT. Ductility in metals includes the material's capability to tolerate plastic deformations before partial or total degradation of its mechanical properties. Modelling this parameter is important in structure and component design because it can be used to estimate material failure under a generic multi-axial stress state. Previous work has attempted to provide accurate descriptions of the mechanical property degradation resulting from the formation, growth, and coalescence of microvoids in the medium. Experimentally, ductile damage is inherently linked with the accumulation of plastic strain; therefore, coupling damage and elastoplasticity is necessary for describing this phenomenon accurately. In this paper, we combine the approach proposed by Lemaitre with the features of an unconventional plasticity model, the extended subloading surface model, to predict material fatigue even for loading conditions below the yield stress.

KEYWORDS. Unconventional plasticity; Ductile damage; Subloading surface; Cyclic loading.

OPEN ACCESS

Citation: Fincato,R., Tsutsumi, S., Numerical modelling of ductile damage mechanics coupled with an unconventional plasticity model, Frattura ed Integrità Strutturale, 38 (2016) 231-236.

Received: 13.05.2016
Accepted: 20.06.2016
Published: 01.10.2016

INTRODUCTION

The degradation of material properties, which results from the initiation of cavities and microcracks induced by large plastic deformations, has been widely studied. Material failure results from microscopic material impurities, which cause the formation and coalescence of microvoids that eventually produce cracks during deformation. Modelling this mechanism is important in many industrial processes for creating optimized reliable designs for structures and components.

There are two main models for the elastoplastic framework [1, 2]: Gurson's void growth model [3] and Lemaitre's model [4, 5], often referred as continuum damage mechanics. Gurson's model is based on void growth, where the plastic yield is inversely proportional to the amount of imperfections; as the porosity increases the material loading decreases. Further studies by Needleman and Tvergaard [6], Koplic and Needleman [7], and Ohata and Toyota [8] extended the damage evolution concept by introducing material parameters to model the acceleration of the degradation of mechanical properties. Lemaitre's theory describes damage as an internal variable and models its evolution with a dissipative potential

that is also a function of the isotropic and kinematic hardening and the temperature. The damage affects the yield function and reduces the stiffness though the definition of the effective stress, first introduced by Kachanov [9].
The main difference between these two approaches is that the void growth model neglects the effect of damage on the elastic behaviour, limiting the softening behaviour during material loading. The present paper uses continuum damage mechanics to describe the damage as an internal variable and aims to couple the ductile damage constitutive equations with those of the subloading surface model, which is an unconventional [10] plasticity theory initially proposed by Hashiguchi [11, 12]. These models combine the advantages of the plasticity model, which describes the accumulation of irreversible contributions during a generic deformation process (i.e., monotonic, non-proportional, cyclic), with the degradation of the mechanical properties because of the large plastic strains.

CONSTITUTIVE EQUATIONS

Subloading surface model

The subloading surface model is regarded as an unconventional plastic model because inelastic contributions can be calculated for every change in the stress state during material loading. This is achieved by removing the separation of elastic and plastic domains, stating that the material always behaves non-linearly. A subloading surface is introduced by a similarity transformation from the conventional plastic potential (i.e., normal-yield surface, Fig. 1). The subloading surface functions as a loading surface always passing through the current stress state and expanding or contracting in the stress space, depending on the loading or unloading of the sample. The analytical expressions for these two surfaces are

$$
\begin{aligned}
&f(\hat{\boldsymbol{\sigma}}) = F(H),\ \hat{\boldsymbol{\sigma}} = \boldsymbol{\sigma} - \boldsymbol{\alpha} &&\text{normal-yield surface}\\
&f(\overline{\boldsymbol{\sigma}}) = RF(H) &&\text{subloading surface}
\end{aligned}
\tag{1}
$$

Here, $\boldsymbol{\sigma}$ is the Cauchy stress, $\boldsymbol{\alpha}$ is the back-stress, F is the isotropic hardening function (defined later), H is the isotropic hardening variable, R is the similarity transformation ratio, and $\overline{\boldsymbol{\sigma}}$ and $\overline{\boldsymbol{\alpha}}$ are the conjugate Cauchy stress and conjugate back-stress for the subloading surface, respectively, which are expressed as

$$
\overline{\boldsymbol{\sigma}} = \boldsymbol{\sigma} - \overline{\boldsymbol{\alpha}},\quad \overline{\boldsymbol{\alpha}} = \mathbf{s} - R\hat{\mathbf{s}},\quad \tilde{\boldsymbol{\sigma}} = \boldsymbol{\sigma} - \mathbf{s},\quad \hat{\mathbf{s}} = \mathbf{s} - \boldsymbol{\alpha}
\tag{2}
$$

The model is extended by the introduction of a mobile similarity centre, $\mathbf{s}$, which moves freely in the stress space following the development of plastic strain. However, some limits are necessary to avoid the similarity centre crossing the plastic potential. This would lead to both theoretical and numerical inconsistencies such as the subloading surface being impossible to define. Therefore, the similarity-centre surface, defined as the locus of points for the similarity centre and its expansion within the normal-yield surface, is limited by a user-defined parameter, χ ($0 < \chi < 1$).

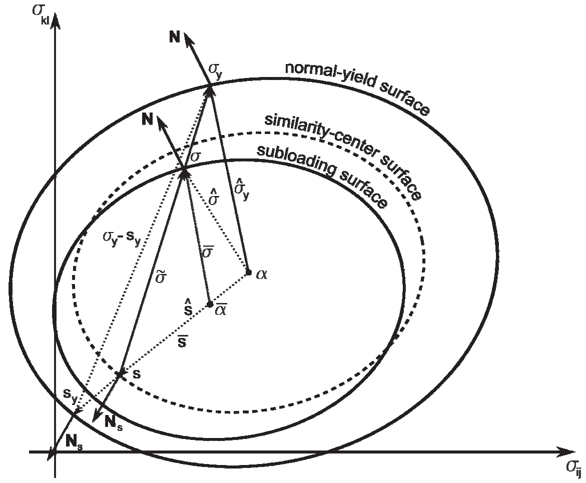

Figure 1: Sketch of the subloading and normal-yield surface.

The mobility of the similarity centre is crucial in the model because it allows material ratcheting to occur during cycles, allowing the prediction of the plastic strain accumulation that is more reliable and realistic, and making the model suitable for fatigue investigation. A detailed explanation of the theoretical features is not the object of this paper and the reader is referred to Refs. [11] and [12] for a more detailed discussion.

Damage

In continuum damage mechanics, the damage variable is assumed to be an internal variable that includes the degradation of the mechanical performance arising from microscale imperfections and defects in the medium. Its evolution is associated with a dissipative mechanism derived from an elastic damage potential [4, 5, 13, 14], and the following assumptions are made.

- The distribution of the defects inside the medium is uniform, which reduces the damage as a scalar isotropic variable.
- Strain equivalence applies, where the strain behaviour is the same for damage or undamaged materials.
- The effective stress, which includes the damage effect on the elastic response that is not included in the Gurson approach, is

$$\boldsymbol{\sigma}^{eff.} = \frac{\boldsymbol{\sigma}}{(1-D)} = \frac{\boldsymbol{\sigma}}{\omega} \tag{3}$$

The coupling with the elastoplastic model is modified by Eq. (1) to include the damage variable, similar to Lemaitre [5], Benallal et al. [15], and De Souza et al. [2] as

$$f(\hat{\boldsymbol{\sigma}}) = \omega F(H); \qquad f(\overline{\boldsymbol{\sigma}}) = \omega R F(H) \tag{4}$$

In contrast to previous studies, the term is not associated with the stress function, ; therefore, the damage variable will not modify the original definition of the outward normal vector in the associated flow rule, simplifying the derivation of all the variables of the plasticity model. Without describing the details of the mathematical manipulations, the main variables are

$$\begin{aligned} &\overset{\circ}{\mathbf{s}} = c\left|\mathbf{D}^p\right|\left(\frac{\tilde{\boldsymbol{\sigma}}}{R} - \left(\frac{1}{\chi}-1\right)\hat{\mathbf{s}}\right) + \overset{\circ}{\boldsymbol{\alpha}} + \left[\frac{1}{F}\frac{dF}{dH}h - \frac{\dot{D}}{\omega}\right]\hat{\mathbf{s}}; \quad \mathbf{N} = \frac{\overline{\boldsymbol{\sigma}}'}{\left|\overline{\boldsymbol{\sigma}}'\right|}; \quad h = \sqrt{\frac{2}{3}} \\ &M^p = tr\left[\mathbf{N}\left(\frac{1}{F}\frac{dF}{dH}h\,\hat{\boldsymbol{\sigma}} + \mathbf{a} + U\frac{\tilde{\boldsymbol{\sigma}}}{R} + (1-R)c\left|\mathbf{D}^p\right|\left(\frac{\tilde{\boldsymbol{\sigma}}}{R} - \left(\frac{1}{\chi}-1\right)\hat{\mathbf{s}}\right) - \frac{\dot{D}}{\omega}\hat{\boldsymbol{\sigma}}\right)\right] \end{aligned} \tag{5}$$

where **a** is $\overset{\circ}{\alpha} = \mathbf{a}\left|\mathbf{D}^p\right|$, c is a material constant regulating the speed of the similarity centre, and U is a mathematical function for defining the similarity ratio rate according to [12]. The corotational stress rate can be written as a function of the total strain rate as

$$\boldsymbol{\sigma} = \left\{\overline{\mathbf{E}} - \frac{\overline{\mathbf{E}}\mathbf{N} \otimes \overline{\mathbf{E}}\mathbf{N}}{M_p + tr\mathbf{N}\overline{\mathbf{E}}\mathbf{N}}\right\}\mathbf{D} \tag{6}$$

The dash over the elastic constant matrix, **E**, indicates that the elastic behaviour is affected by the damage. The damage evolution law is assumed to be

$$\dot{D} = \frac{\lambda^+}{\omega}\left(\frac{Y}{s_1}\right)^{s2}\left\langle H - s_3\right\rangle; \quad Y = -\left[\frac{f(\overline{\boldsymbol{\sigma}})^2}{6G\omega^2} + \frac{\overline{\sigma}_m^2}{2K\omega^2}\right]; \quad \begin{cases} \overline{\sigma}_m > 0 \rightarrow \lambda^+ > 0 \ and\ \dot{D} > 0 \\ \overline{\sigma}_m \le 0 \rightarrow \lambda^+ = 0 \ and\ \dot{D} = 0 \end{cases} \tag{7}$$

where λ is the plastic multiplier and superscript + indicates that just the tensile contributions are considered. s_1, s_2, and s_3 are material parameters; s_1 and s_2 affect the energy release rate, Y [2, 5], and s_3 is a threshold for the cumulative plastic strain after which damage begins (the term in the Macaulay brackets is null until H = s_3). σ_m is the mean stress and *G* and *K* are the shear and bulk moduli, respectively.

NUMERICAL TESTS

The constitutive equations were implemented in commercial finite element code, Abaqus 6.14, via a user subroutine, and they were used to simulate a monotonic extension of an A533B steel bar. A similar numerical and experimental test was conducted by Bonora et al. [1], and it was used as a reference for our simulation. The sample geometry and boundary conditions were taken from the literature (Fig. 2). For simplicity, one eighth of the sample was modelled, applying symmetric constraints on the cut sections. For the mesh discretization, 7870 linear brick elements were used for 9548 nodes.

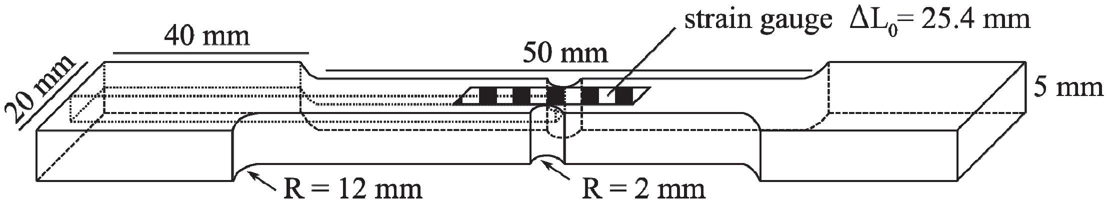

Figure 2: Sketch of the steel bar (grey area indicates the modelled portion).

The material parameters were obtained from the calibration uniaxial extension test in Fig. 7 and they are reported in Tab. 1.

E	200 GPa
ν	0.3
F_0	345 MPa
h_1, h_2	1.0; 11
c, χ	200; 0.9
s_1, s_2, s_3	2.5; 1.0; 0.65

Table 1: A533B steel material parameters for the subloading surface model.

The kinematic hardening contribution was neglected and the following isotropic hardening law was used.

$$F = F_0\left[1 + h_1\left\{1 - e^{(-h_2 H)}\right\}\right], \quad \frac{dF}{dH} = F_0\, h_1\, h_2\, e^{(-h_2 H)} \tag{8}$$

The s3 damage parameter in the first of Eqs. (7) is set to activate the damage after the cumulative isotropic hardening variable, H, reaches a threshold of 65%, and an element deletion occurs whenever the damage variable is 0.70 at the Gauss point, which is assumed as a critical value for void coalescence and crack formation.
Fig. 4–6 show the damage contour fields before and after the first crack formation, and near the end of the analysis. The crack is initiated corresponding to the notch, but not at the surface, and it rapidly propagates in the centre of the cross section in accordance with the results obtained by Bonora et al. [1]. This can be explained by the competition between the stress triaxiality and the plastic strains, which both affect the damage variable as shown in Eq. (7). The evolution of these two element entities in the cross section of Fig. 3 shows that the stress triaxiality is higher at the bar core (point B) than on the surface (point A), whereas the opposite is observed for the cumulative plastic strain (Fig. 9 and 10).

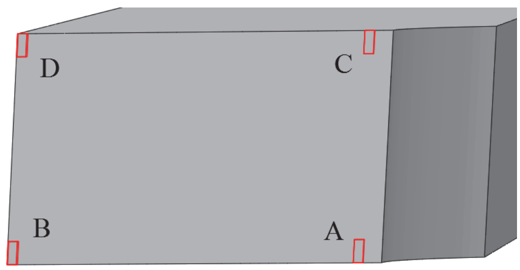

Figure 3: Reference elements in the central cross section.

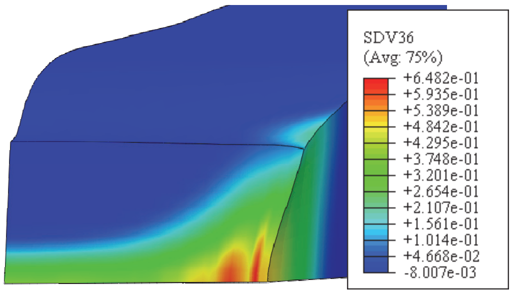

Figure 4: Damage contour field before crack opening (axial strain = 0.1670).

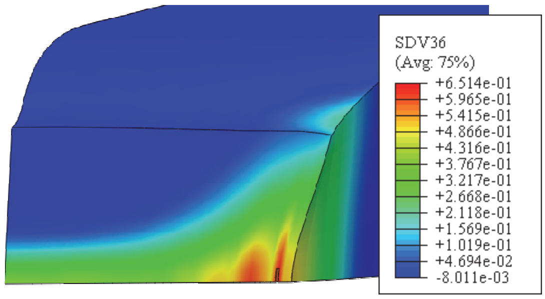

Figure 5: Damage contour field at the crack opening (axial strain = 0.1675).

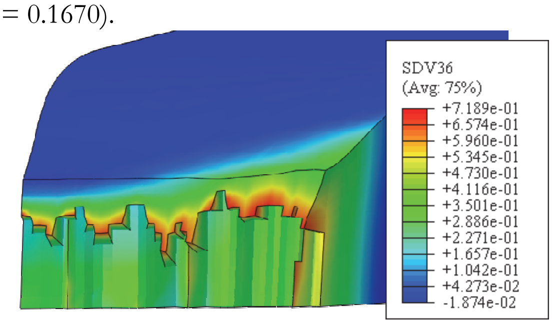

Figure 6: Damage contour field at the end of computation (axial strain = 0.1756).

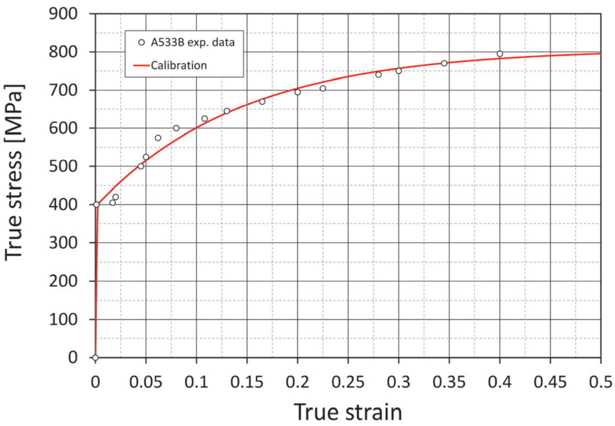

Figure 7: Material calibration parameter.

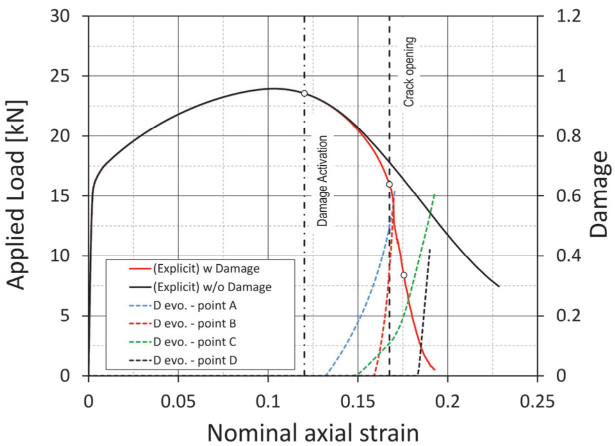

Figure 8: Applied load vs nominal axial strain.

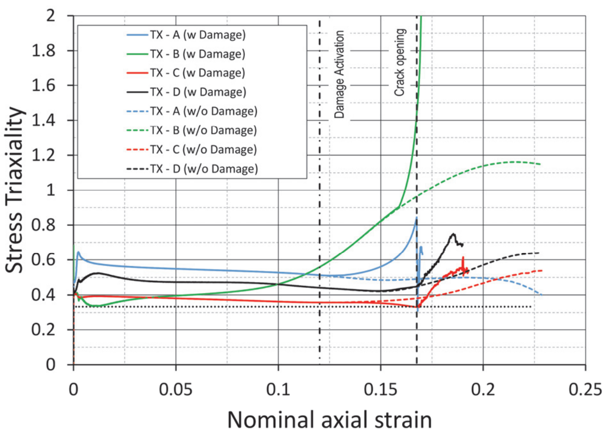

Figure 9: Stress triaxiality in the reference elements in Fig. 3.

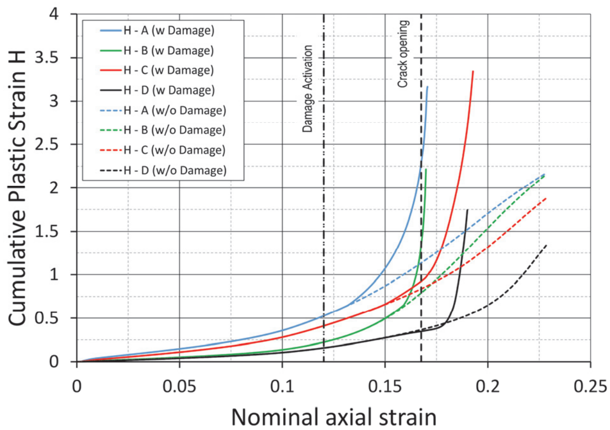

Figure 10: *H* evolution in the reference elements in Fig. 3.

Therefore, the crack opens in an intermediate position, closer to the factor that is predominant, which is the deformation in this case. In addition, the graphs show the curves obtained without considering the damage, to highlight the effect of the coupling.
Fig. 8 shows the applied forces as a function of the nominal strain measured at the same point on the strain gauge as in Fig. 2. The damage solution agrees well with the solution reported by Bonora et al. [1] showing the complete rupture of the sample at a nominal axial strain of 15%–20%. Between the damage activation and the first crack opening, the red curve shows a small gap for the no damage solution (black line), interpreted as the microvoid formation mechanism. Corresponding to the crack opening, a large decrease is observed, leading to sudden material failure. The damage evolution shows that the fracture starts closer to the surface, although the propagation in the core towards point B is fast, whereas it is slower on the external surface (points C and D).

CONCLUSIONS

We performed a monotonic tensile test with a coupled elastoplastic and damage model within the framework of continuum damage mechanics. Following the approach proposed by Lemaitre, the concept of damage as an internal variable was included in an unconventional plasticity model to simulate of the degradation of the mechanical properties in metals during non-linear analyses.
The model was used to investigate the behaviour of a notched steel bar undergoing monotonic uniaxial extension. The results showed good agreement with the reference solution in the literature Bonora et al. [1], indicating that the coupled constitutive equations were implemented correctly. To take advantage of the subloading surface model features, the numerical algorithm will be applied to cyclic loading to study the effect of damage on fatigue tests.

REFERENCES

[1] Bonora, N., Gentile, D., Pirondi, A., Newaz, G. Ductile damage evolution under triaxial state of stress: theory and experiments, Int. J. Plast., 21(2005) 981-1007. doi:10.1016/j.ijplas.2004.06.003.
[2] De Souza, E.N., Peric, D., Owen, D.J.R., Computational Methods for Plasticity, John Wiley and Sons, Chichester (2008) 471-515.
[3] Gurson, A.L., Continuum theory of ductile rapture by void nucleation and growth: part I – yield criteria and flow rules for porous ductile media, J. Eng. Mat. Tech., 99(1977), 2-15. doi:10.1115/1.3443401.
[4] Lemaitre, J., A continuous damage mechanics model for ductile fracture, J. Engng. Mat. Tech., 107 (1985) 83-89. doi:10.1115/1.3225775.
[5] Lemaitre, J., Coupled elasto-plasticity and damage constitutive equations, Compt. Meth. Appl. M., 51 (1985) 31-49. doi:10.1016/0045-7825(85)90026-X.
[6] Needleman, A., Tvergaard, V. An analysis of ductile rapture in notched bars, J. Mech. Phys. Solids., 32(1984) 461. doi:10.1016/0022-5096(84)90031-0.
[7] Koplik, J., Needleman, A., Void Growth and coalescence in porous plastic solids, Int. J. Solids Struct., 24(1988), 835-853. doi:10.1016/0020-7683(88)90051-0.
[8] Ohata, M., Toyoda, M., Damage concept for evaluating ductile cracking of steel structure subjected to large-scale cyclic straining, Sci. Technol. Adv. Mat., 5(2004), 241-249.
[9] Kachanov, L.M., In: Introduction to Continuum Damage Mechanics, Martinus, Nijhoff Publisher (Ed.), Boston-Dordrecht (1986).
[10] Drucker, D.C., Conventional and unconventional plastic response and representation, Appl. Mech. Rev. ASME, 41(1988) 151-167. doi:10.1115/1.3151888.
[11] Hashiguchi, K., Subloading surface model in unconventional plasticity, Int. J. Solids Struct., 25(1989), 917-945. doi:10.1016/0020-7683(89)90038-3.
[12] Hashiguchi, K., In: Elastoplasticity theory. Lecture notes in applied and computational mechanics, F. Pfeiffer, P. Wriggers (Eds.), Springer, Berlin, Germany, 42 (2009).
[13] Lemaitre, J., Chaboche, J.L., In: Mechanics of Solids Materials, Cambdrige University Press (1990).
[14] Lemaitre, J., In: A course on damage mechanics, Berlin, Heidelberg, New York: Springer (1996).
[15] Benallal, A., Billardon, R., Lemaitre, J., Continuum damage mechanics and local approach to fracture: Numerical procedures, Compt. Meth. Appl. M., 92 (1989) 141-155. doi:10.1016/0045-7825(91)90236-Y.